Copy 5
RM L52D28

NACA RM L52D28

NACA

RESEARCH MEMORANDUM

THE AERODYNAMIC CHARACTERISTICS AT TRANSONIC SPEEDS OF AN ALL-MOVABLE, TAPERED, 45° SWEPTBACK, ASPECT-RATIO-4 TAIL SURFACE DEFLECTED ABOUT A SKEWED HINGE AXIS

By Alexander D. Hammond and James M. Watson

Langley Aeronautical Laboratory
Langley Field, Va.

NATIONAL ADVISORY COMMITTEE
FOR AERONAUTICS

WASHINGTON

July 3, 1952

NATIONAL ADVISORY COMMITTEE FOR AERONAUTICS

RESEARCH MEMORANDUM

THE AERODYNAMIC CHARACTERISTICS AT TRANSONIC SPEEDS OF AN ALL-MOVABLE, TAPERED, 45° SWEPTBACK, ASPECT-RATIO-4 TAIL SURFACE DEFLECTED ABOUT A SKEWED HINGE AXIS

By Alexander D. Hammond and James M. Watson

SUMMARY

An investigation was made at transonic speeds in the Langley high-speed 7- by 10-foot tunnel to determine the hinge-moment and other aerodynamic characteristics of an all-movable, 6-percent-thick, tapered, 45° sweptback, aspect-ratio-4 tail surface deflected about a skewed hinge axis. The investigation was extended through the transonic speed range by testing in the high velocity field over a reflection plane on the side wall of the tunnel.

The pitching- and hinge-moment coefficients against lift coefficient are generally linear and independent of the way the lift coefficient was obtained.

The variation of hinge-moment coefficient with control deflection and angle of attack can be calculated from the basic aerodynamic data for the tail surface.

The hinge-moment characteristics of this tail pivoted about a skewed axis are somewhat improved over the hinge-moment characteristics of the tail pivoted about a normal axis.

INTRODUCTION

Flap-type controls have in some cases shown undesirable characteristics near the speed of sound such as large, erratic, and unpredictable control deflections required for trim at these speeds. The use of all-movable tail surfaces with the hinge axis normal to the plane of symmetry has improved somewhat the undesirable variation of control deflection for trim but still presents the problem of large changes in hinge moments near the speed of sound.

A study of the aerodynamic characteristics of a sweptback tail revealed that the center of pressure moves outboard as well as rearward with increase in Mach number. With this in mind it was thought that, if an all-movable tail were pivoted about a skewed axis parallel with the locus of the centers of pressure, an improvement in the hinge-moment characteristics could be realized.

Available basic data (ref. 1) were used to estimate the locus of the centers of pressure on an aspect-ratio-4, taper-ratio-0.6, 45° sweptback all-movable tail. The present investigation presents the aerodynamic and hinge-moment characteristics of this tail pivoted about an axis corresponding to the 20-percent-chord line, which is slightly ahead of the locus of the centers of pressure through the Mach number range up to a Mach number of 1.1. The purpose of the present paper was to determine whether the characteristics about a skewed axis could be predicted from data about the normal angle-of-attack axis, and whether such a configuration offered any aerodynamic advantages over the conventional hinge location normal to the plane of symmetry.

SYMBOLS

C_L lift coefficient, $\dfrac{\text{Twice lift of semispan model}}{qS}$

C_m pitching-moment coefficient referred to $0.25\bar{c}$, $\dfrac{\text{Twice pitching moment of semispan model}}{qS\bar{c}}$

C_B bending-moment coefficient at plane of symmetry, $\dfrac{\text{Root bending moment}}{q\frac{S}{2}\frac{b}{2}}$

C_h hinge-moment coefficient about hinge line, $\dfrac{\text{Twice hinge moment of semispan model}}{qS\bar{c}}$

q effective dynamic pressure over span of model, $\frac{1}{2}\rho V^2$, lb/sq ft

S twice area of semispan model, 0.125 sq ft

$\bar{c}$ mean aerodynamic chord, $\frac{2}{S}\int_0^{b/2} c^2 dy$, 0.1805 ft on model

c	local wing chord, ft
b	twice span of semispan model, 0.7071 ft
y	spanwise distance from plane of symmetry, ft
ρ	mass density of air, slugs/cu ft
V	average free-stream air velocity, ft/sec
M	effective Mach number over span of model
M_a	average chordwise local Mach number
M_l	local Mach number
R	Reynolds number of model based on $\bar{c}$
α	angle of attack, deg; measured in plane of symmetry
A	aspect ratio, b^2/S, 4.0 on model
δ	deflection of model about 20-percent-chord line, deg; positive when trailing edge is down
Λ_{HL}	angle of sweep of hinge line
$\delta \cos \Lambda_{HL}$	change in angle of attack at root-chord line caused by change in tail deflection about hinge line

The forces and moments on the tail are presented relative to the axes shown in figure 1. Tail deflections and tail hinge moments were measured about an axis which corresponds to the 20-percent-chord line. All other forces and moments and the angles of attack were measured relative to the wind axes (fig. 1) which, for zero angle of attack and deflection, intersect at the plane of symmetry and the chord plane of the tail at the 25-percent mean-aerodynamic-chord station, as shown in figure 2.

MODEL AND APPARATUS

The all-movable tail used in the investigation had an aspect ratio of 4, a taper ratio of 0.6, sweepback of 45° at the quarter-chord line, and an NACA 65A006 airfoil section parallel to the free stream. The tail was made of steel and was constructed to the plan-form dimensions shown in figure 2.

The data were obtained in the Langley high-speed 7- by 10-foot tunnel with the model mounted on a reflection plane in a manner similar to that described in reference 2. At a given tail deflection the model was restrained from rotating about the 20-percent-chord line by an electrical strain gage secured to a shaft extending the hinge axis through the reflection plane. The model was deflected about the 20-percent-chord line by releasing the strain gage mentioned above, deflecting the model, and relocking the strain gage.

The tail was arranged so that no gap occurred between the reflection plane and the model when the tail was deflected and was sealed by a sponge seal fastened to the reflection-plane turntable to minimize leakage around the tail butt. The model was mounted as shown in figure 3.

Force and moment measurements were obtained on an electrical strain-gage-balance system.

TESTS

The tests were made in the Langley high-speed 7- by 10-foot tunnel. Typical contours showing the Mach number distribution over the side-wall reflection plane in the vicinity of the model are presented in figure 4. Effective test Mach numbers were obtained from contour charts similar to those shown in figure 4 by the relationship

$$M = \frac{2}{S}\int_0^{b/2} cM_a \, dy$$

For these tests a Mach number gradient of generally less than 0.02 was obtained below a Mach number of 0.95, and the gradient increased to about 0.05 at the higher test Mach numbers.

The angles of attack were measured in a plane perpendicular to a normal axis through the quarter chord of the mean aerodynamic chord, and the tail deflections were measured in a plane perpendicular to the 20-percent-chord line. The model was symmetrical; therefore, to reduce the number of model changes and the tunnel time, the force and the moment measurements were taken through an angle-of-attack range from -20° to 20° and at tail deflections from 0° to -30°. These measurements were then considered, with due regard to sign, to be equivalent to the measurements that would be obtained if taken through an angle-of-attack range from 0° to 20° and at tail deflections from -30° to 30°. The measurements taken in the negative angle-of-attack range provided the measurements for the positive deflections. The pitching-moment data are

presented about a normal axis through the quarter chord of the mean aerodynamic chord. The bending moments are presented about the root-chord line, and the hinge moments are presented about the 20-percent-chord line. These measurements were obtained from a Mach number of 0.611 to about 1.058. The variation of Reynolds number with Mach number is presented in figure 5.

In view of the small size of the tail relative to the tunnel test section, jet-boundary and blockage corrections were believed to be insignificant and were not applied to the data.

DISCUSSION

The basic data obtained from tests of an all-movable, 45° sweptback, aspect-ratio-4, taper-ratio-0.6 tail deflected about the 20-percent-chord line are presented in figure 6 against tail deflection at various angles of attack and Mach numbers. Sealing of the gap around the root of the model is in contrast to a practical installation where relatively large gaps might occur at the tail root when the tail surface is deflected about the 20-percent-chord line.

The slopes of lift coefficient against tail deflection (fig. 6) remain about constant through the angle-of-attack range investigated. The slopes of the bending-moment coefficient against tail deflection remain about constant through 12° angle of attack. Above an angle of attack of 12° the values of these slopes increase.

The angle of attack in the plane of symmetry caused by deflection of the tail is approximated by $\delta \cos \Lambda_{HL}$ and the total angle of attack in the plane of symmetry is $\alpha + \delta \cos \Lambda_{HL}$. All the lift-coefficient data were plotted against the angle of attack in the stream direction $\left(\alpha + \delta \cos \Lambda_{HL}\right)$ in figure 7, and all the pitching-moment and hinge-moment coefficients are presented against lift coefficient in figure 8. Although there was appreciable dihedral involved when the model was pivoted about the 20-percent-chord line, these figures show that the dihedral effect on the characteristics was negligible. From the data shown in figure 7 it can be seen that the lift coefficient is dependent only upon the resultant change in angle of attack of the root-chord line of the tail and is independent of whether the tail is deflected about the normal axis through $0.25\bar{c}$ or about the 20-percent-chord line. Figure 8 indicates that the variations of pitching-moment and hinge-moment coefficients are generally linear in the low and moderately high lift-coefficient range and are dependent only upon the lift coefficient. At a given lift coefficient and Mach number, therefore, these moments are independent of how

the lift coefficient was obtained. In addition, figures 7 and 8 show that the basic aerodynamic data through the angle-of-attack range are sufficient to calculate the hinge-moment coefficients that would be obtained if this tail were pivoted about a skewed axis.

The variation of the hinge-moment coefficient with lift coefficient of the all-movable tail, if it were pivoted about a normal axis, is shown by the variation of C_m with C_L in figure 8. An analysis of the data of figure 8 indicates that the tail pivoted about a normal axis would have undesirable stick forces that decrease with increase in lift coefficient above 0.5 to 0.6 C_L. However, the variation of hinge moments of an all-movable tail pivoted about the 20-percent-chord line (fig. 8) indicates that the stick force on the tail would increase with increase in C_L throughout the lift-coefficient range investigated. Rearward movement of the normal axis to reduce the hinge-moment coefficients through the Mach number range would cause the variation of C_m with C_L (and, therefore, the stick forces) to become even more undesirable (fig. 8). The stick forces for the tail pivoted about the 20-percent-chord line are in the right direction throughout the lift-coefficient range; therefore, this axis could be moved nearer the locus of the centers of pressure to reduce the hinge-moment coefficients through the Mach number range.

A diagram showing the relative locations of the centers of pressure through the Mach number range, the 20-percent-chord line, the 26-percent-chord line, and the normal axis is presented in figure 9. Also shown in figure 9 is the variation of C_h/C_L (obtained from the curves of C_m against C_L in fig. 8) of an all-movable tail pivoted about the normal axis, C_h/C_L for the tail pivoted about the 20-percent-chord line, and estimated values of C_h/C_L for the tail pivoted about the 26-percent-chord line.

The variation of C_h/C_L presented in figure 9 indicates that this tail pivoted about the 26-percent-chord line, near the locus of centers of pressure, would have improved hinge-moment characteristics throughout the lift-coefficient and Mach number range over those for the tail pivoted about the normal axis.

CONCLUSIONS

An investigation was made in the Langley high-speed 7- by 10-foot tunnel to determine the aerodynamic characteristics and hinge moments

of an all-movable, 45° sweptback, aspect-ratio-4, taper-ratio-0.6 tail deflected about a skewed hinge axis. The following conclusions may be drawn from the data:

1. The variation of the pitching- and hinge-moment coefficients with lift coefficient are generally linear and independent of the way the lift coefficient was obtained.

2. Basic aerodynamic data through the angle-of-attack range are sufficient to calculate the hinge-moment coefficients that would be obtained if this tail were pivoted about a skewed axis.

3. The all-movable tail pivoted about a skewed axis near the locus of the centers of pressure would have improved hinge-moment characteristics throughout the lift-coefficient and Mach number range investigated over the hinge-moment characteristics of the tail pivoted about an axis normal to the plane of symmetry.

Langley Aeronautical Laboratory
National Advisory Committee for Aeronautics
Langley Field, Va.

REFERENCES

1. Sleeman, William C., Jr., Klevatt, Paul L., and Linsley, Edward L.: Comparison of Transonic Characteristics of Lifting Wings From Experiments in a Small Slotted Tunnel and the Langley High-Speed 7- by 10-Foot Tunnel. NACA RM L51F14, 1951.

2. Spreemann, Kenneth P., and Alford, William J., Jr.: Small-Scale Investigation at Transonic Speeds of the Effects of Thickening the Inboard Section of a 45° Sweptback Wing of Aspect Ratio 4, Taper Ratio 0.3, and NACA 65A006 Airfoil Section. NACA RM L51F08a, 1951.

[redacted]

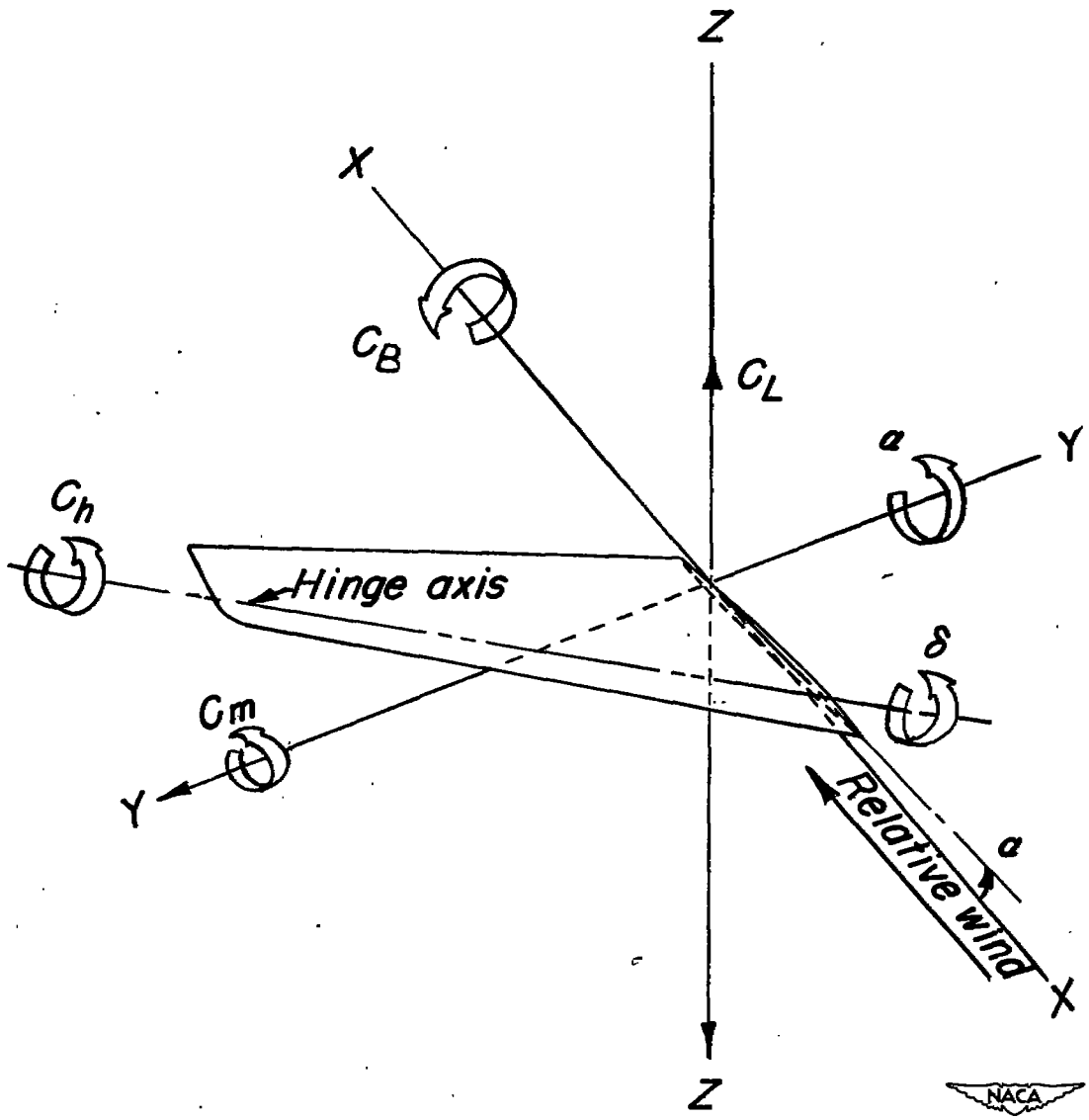

Figure 1.- System of axes, tail hinge moments, and deflections. Positive directions of forces, moments, and deflections are indicated by the arrows.

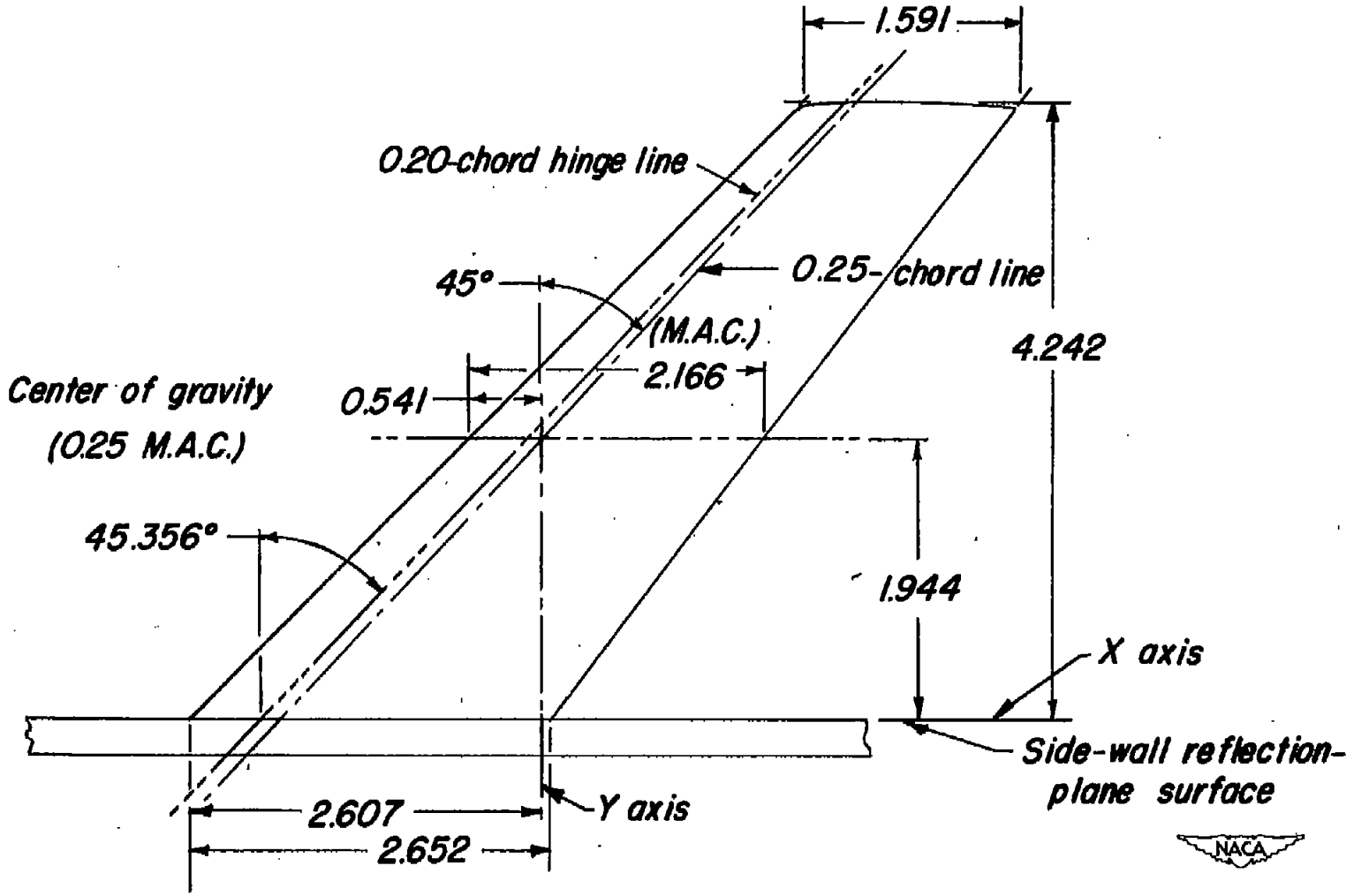

Figure 2.- Plan form and dimensions of the aspect-ratio-4, taper-ratio-0.6, 45° sweptback all-movable tail. All dimensions are in inches unless otherwise noted.

Figure 3.- Typical model mounted on the side-wall reflection plane in the Langley high-speed 7- by 10-foot tunnel.

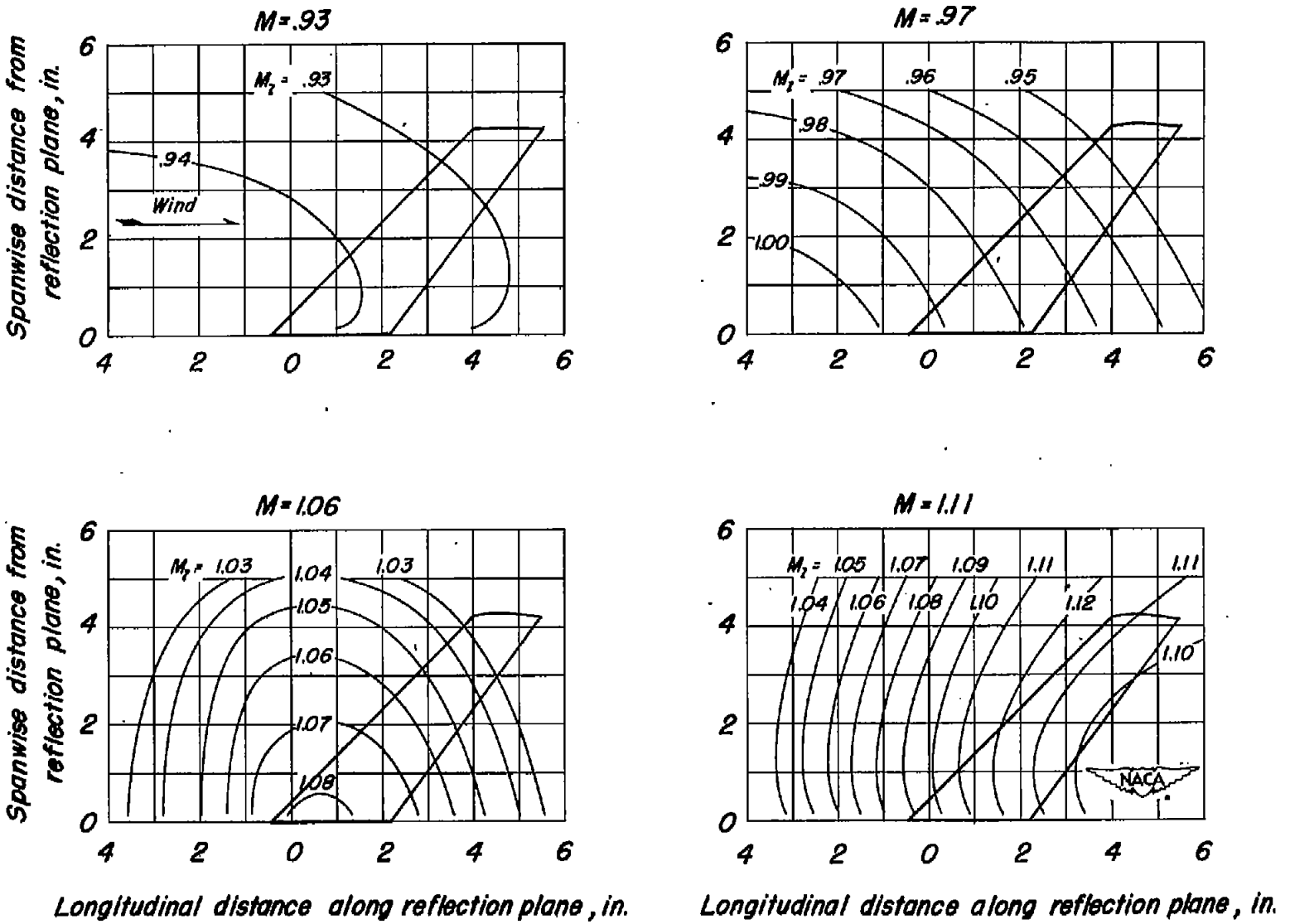

Figure 4.- Typical Mach number contours obtained over the all-movable tail.

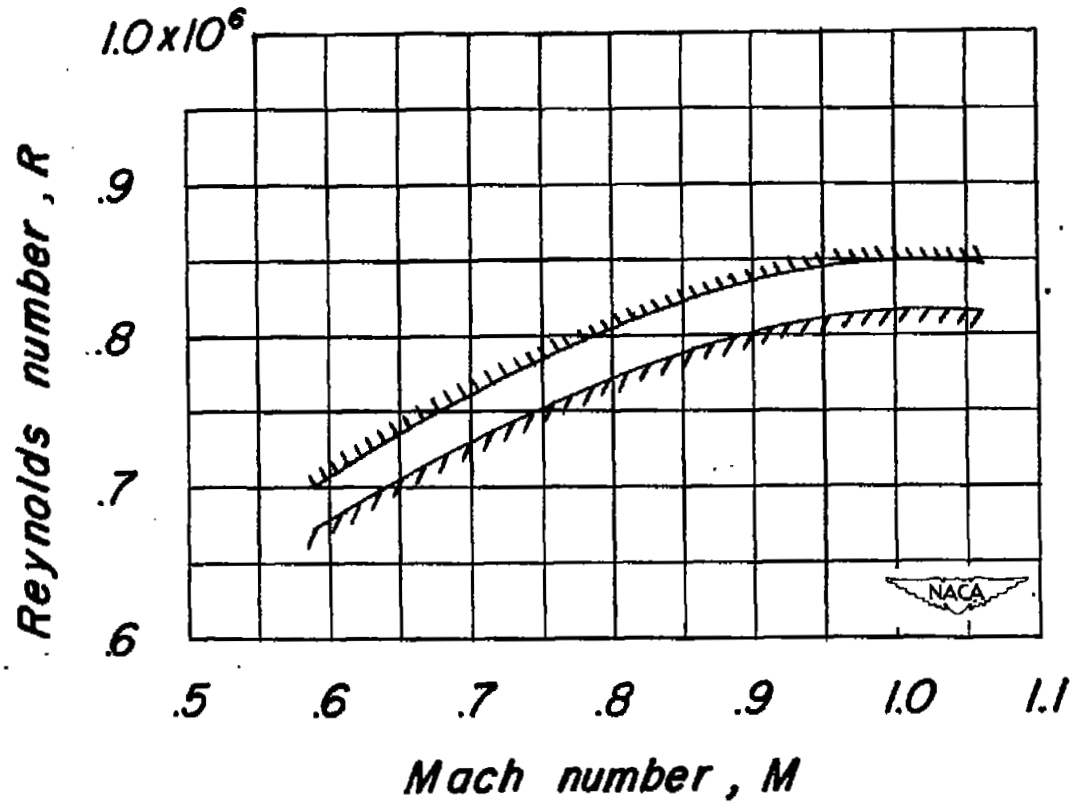

Figure 5.- The variation of Reynolds number with Mach number for tests of the all-movable tail.

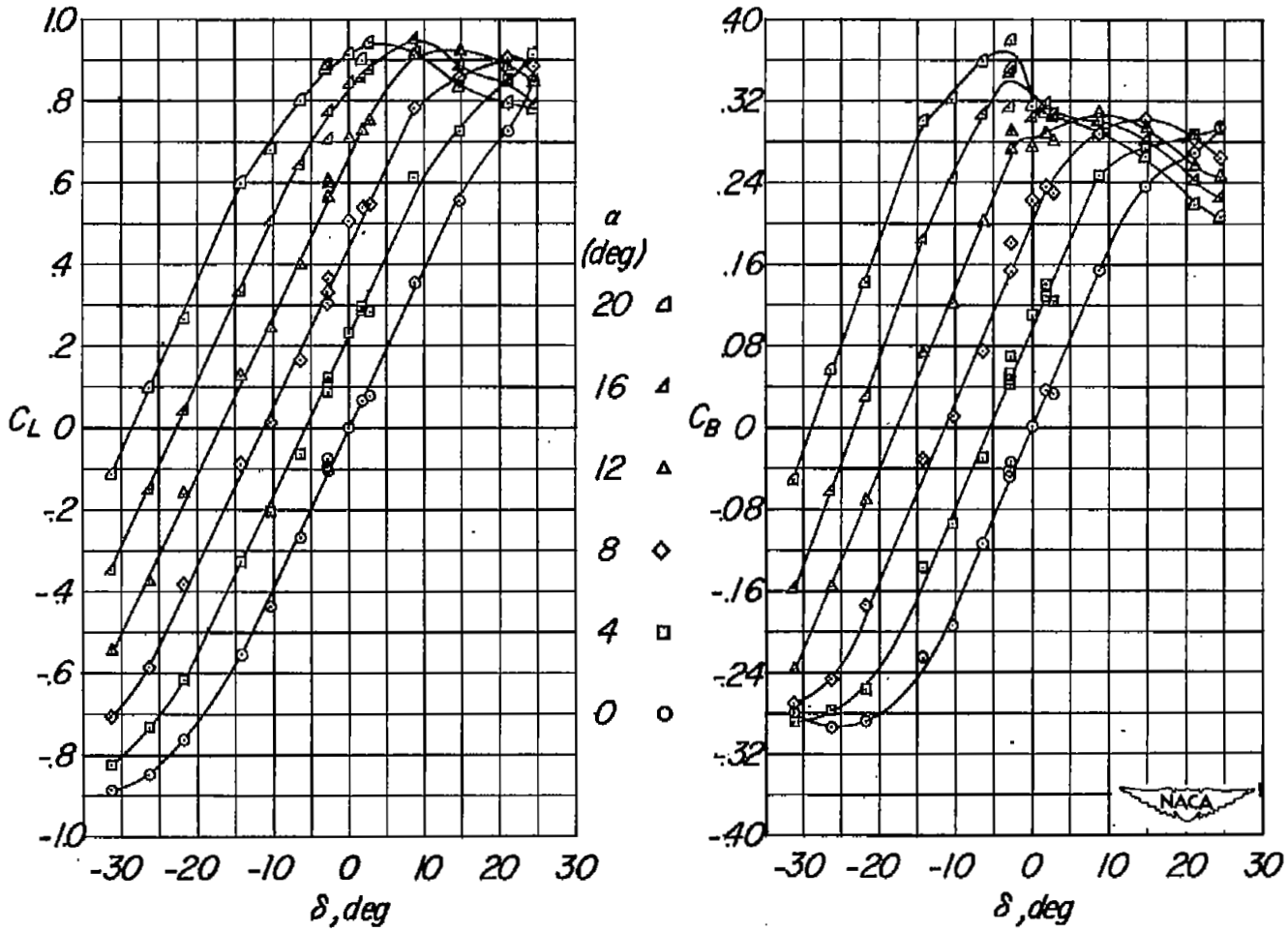

(a) Mach number, 0.611.

Figure 6.- The aerodynamic characteristics at various angles of attack of the aspect-ratio-4, taper-ratio-0.6, 45° sweptback all-movable tail against tail deflection about the 0.20-chord line.

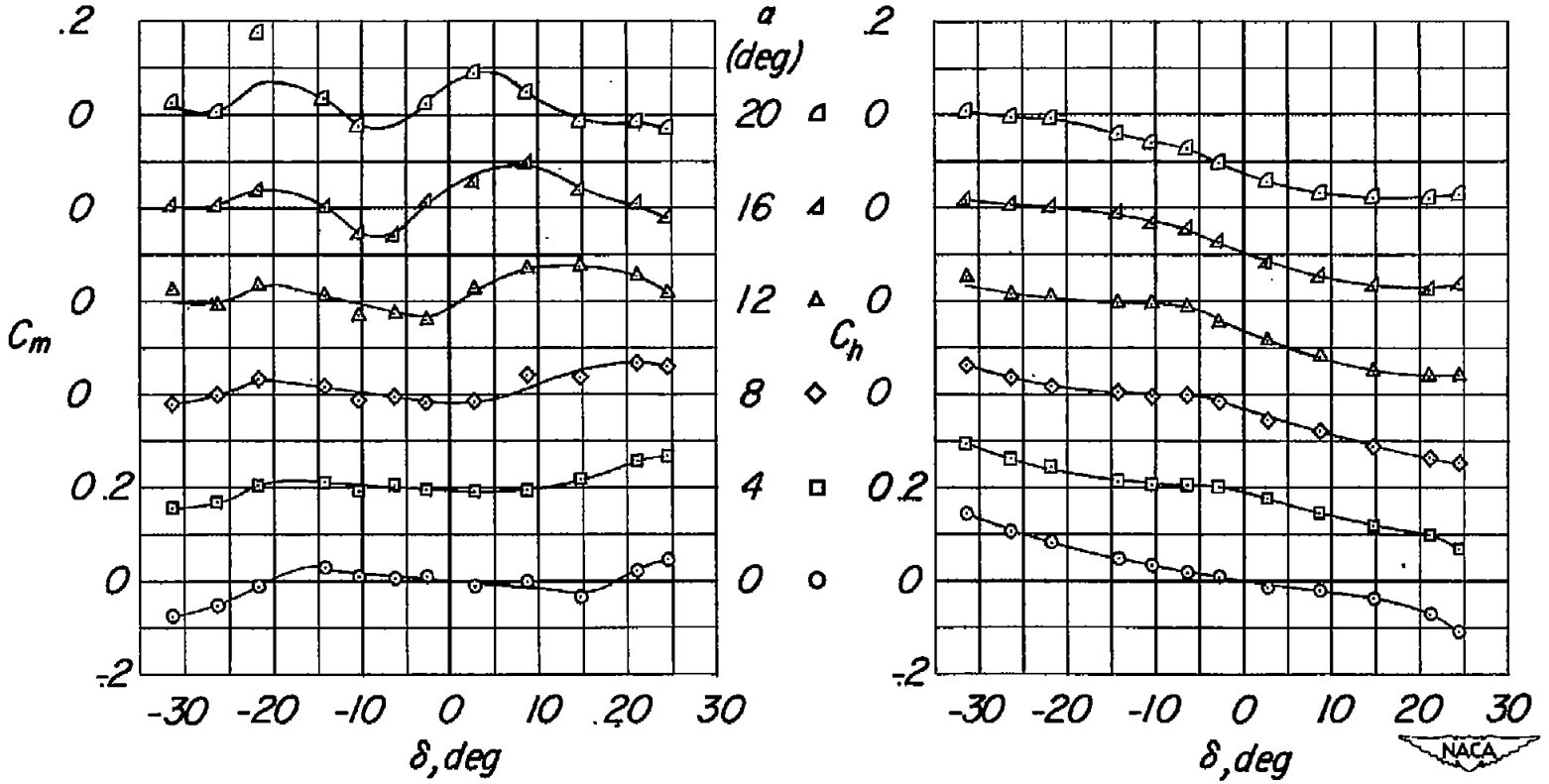

(a) Concluded.

Figure 6.- Continued.

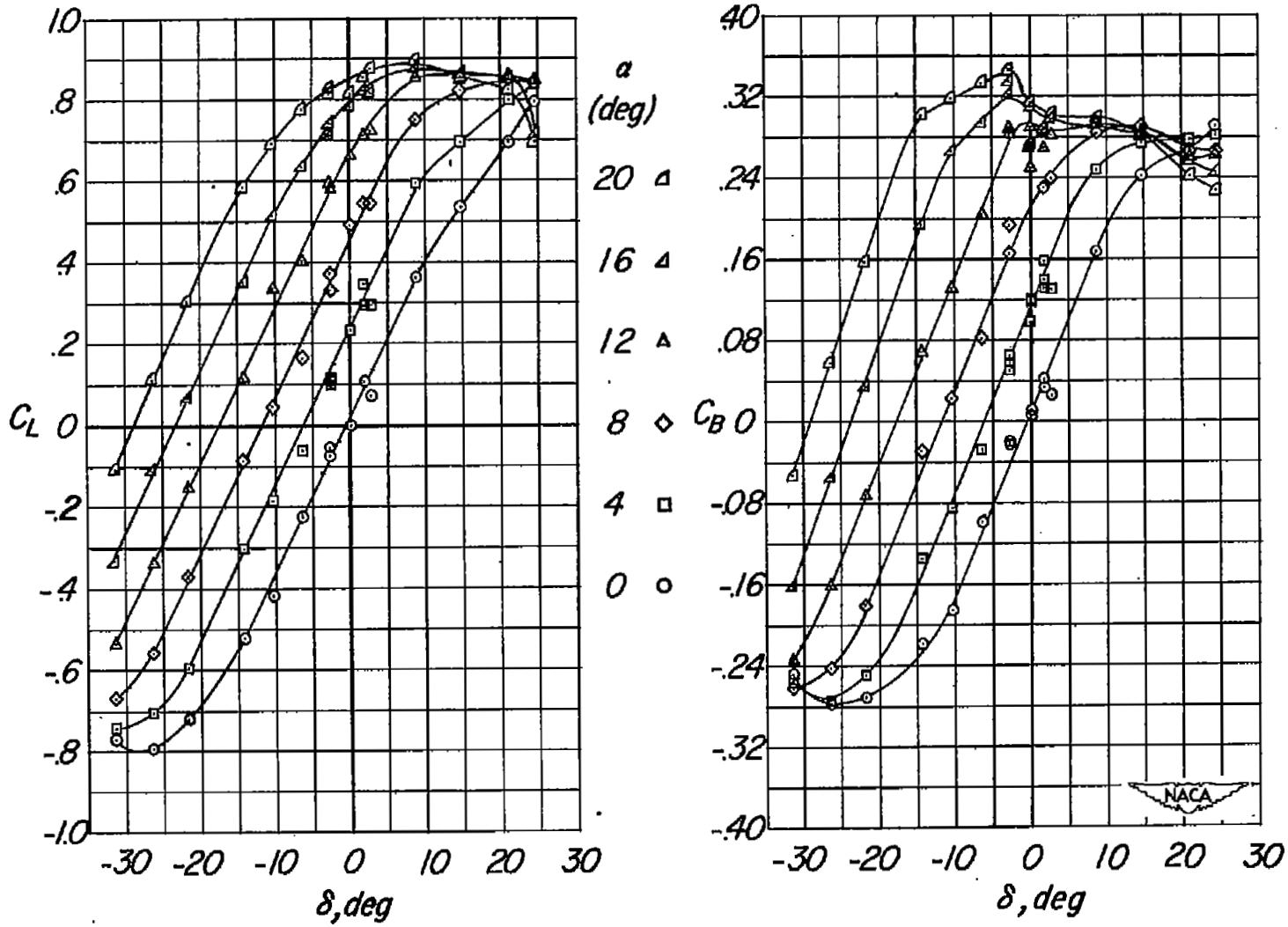

(b) Mach number, 0.816.

Figure 6.- Continued.

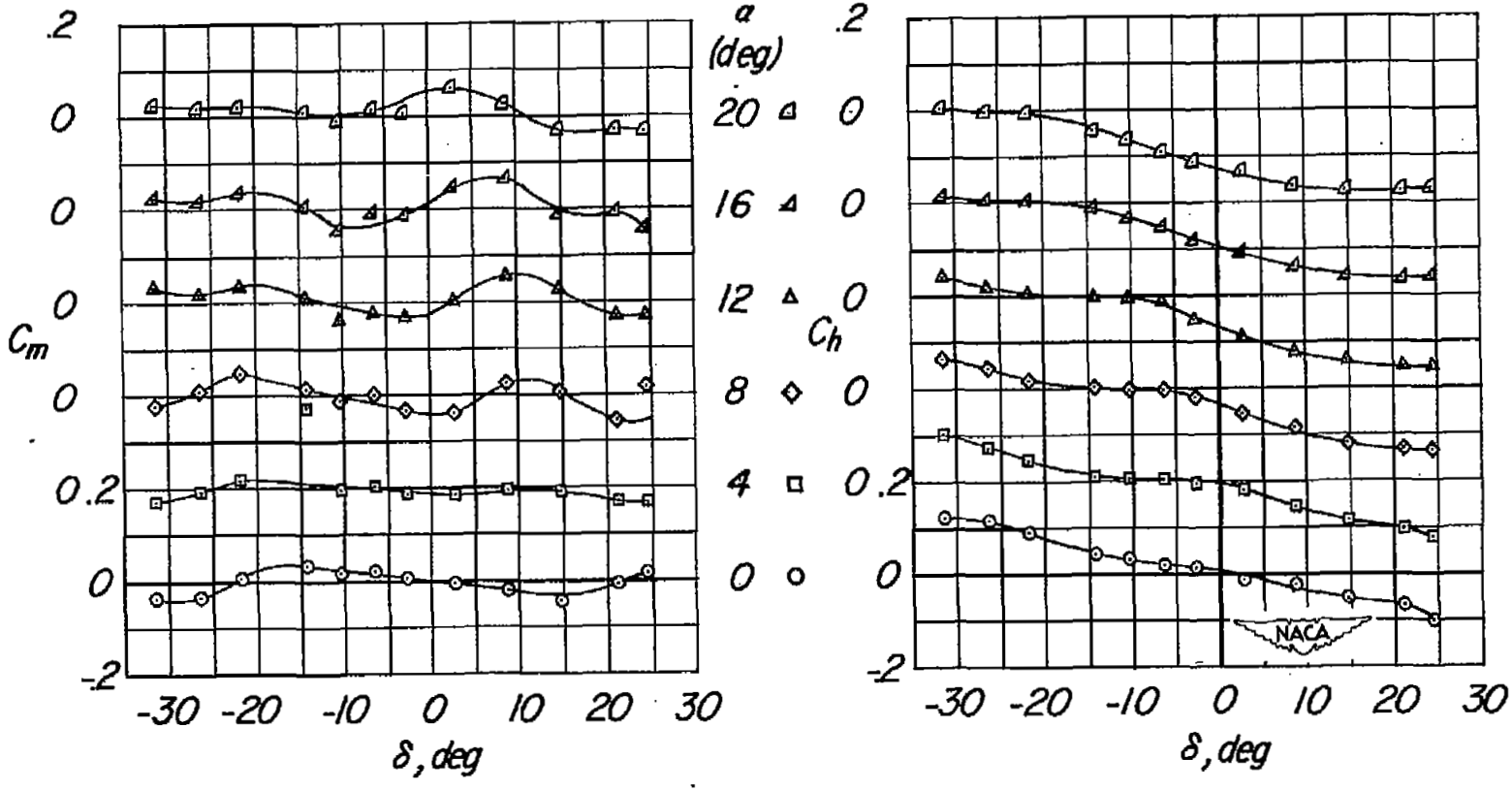

(b) Concluded.

Figure 6.- Continued.

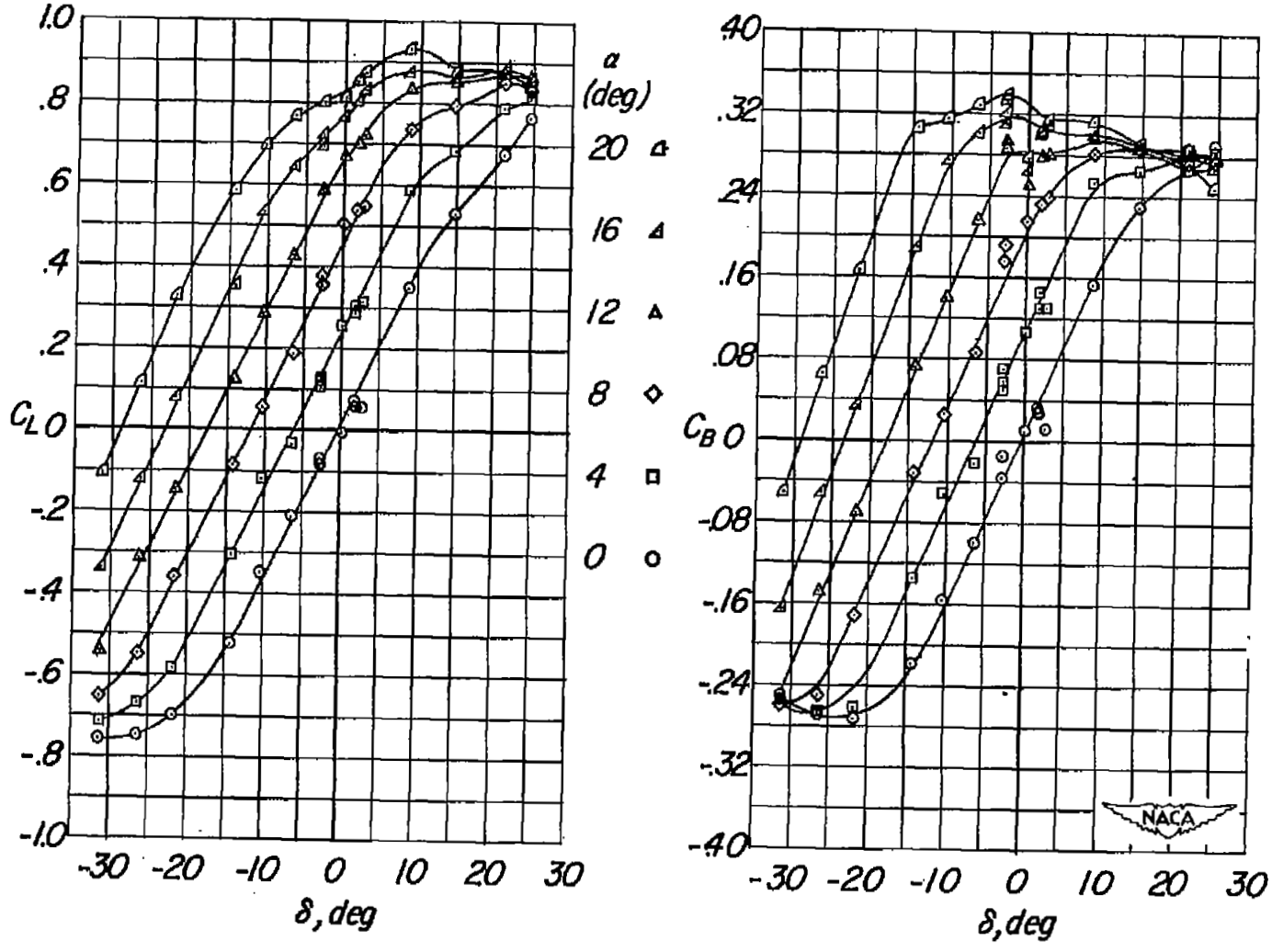

(c) Mach number, 0.920.

Figure 6.- Continued.

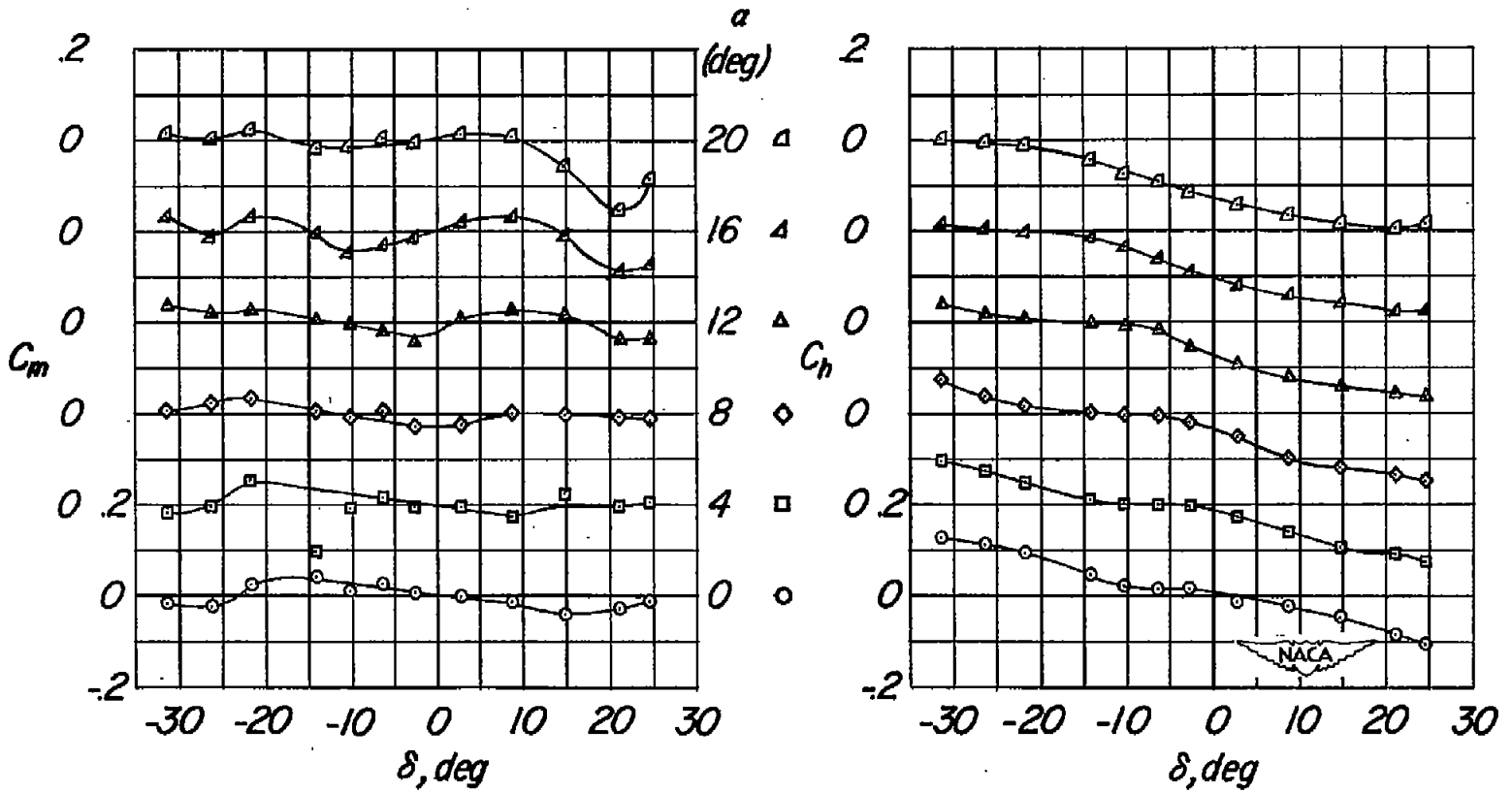

(c) Concluded.

Figure 6.- Continued.

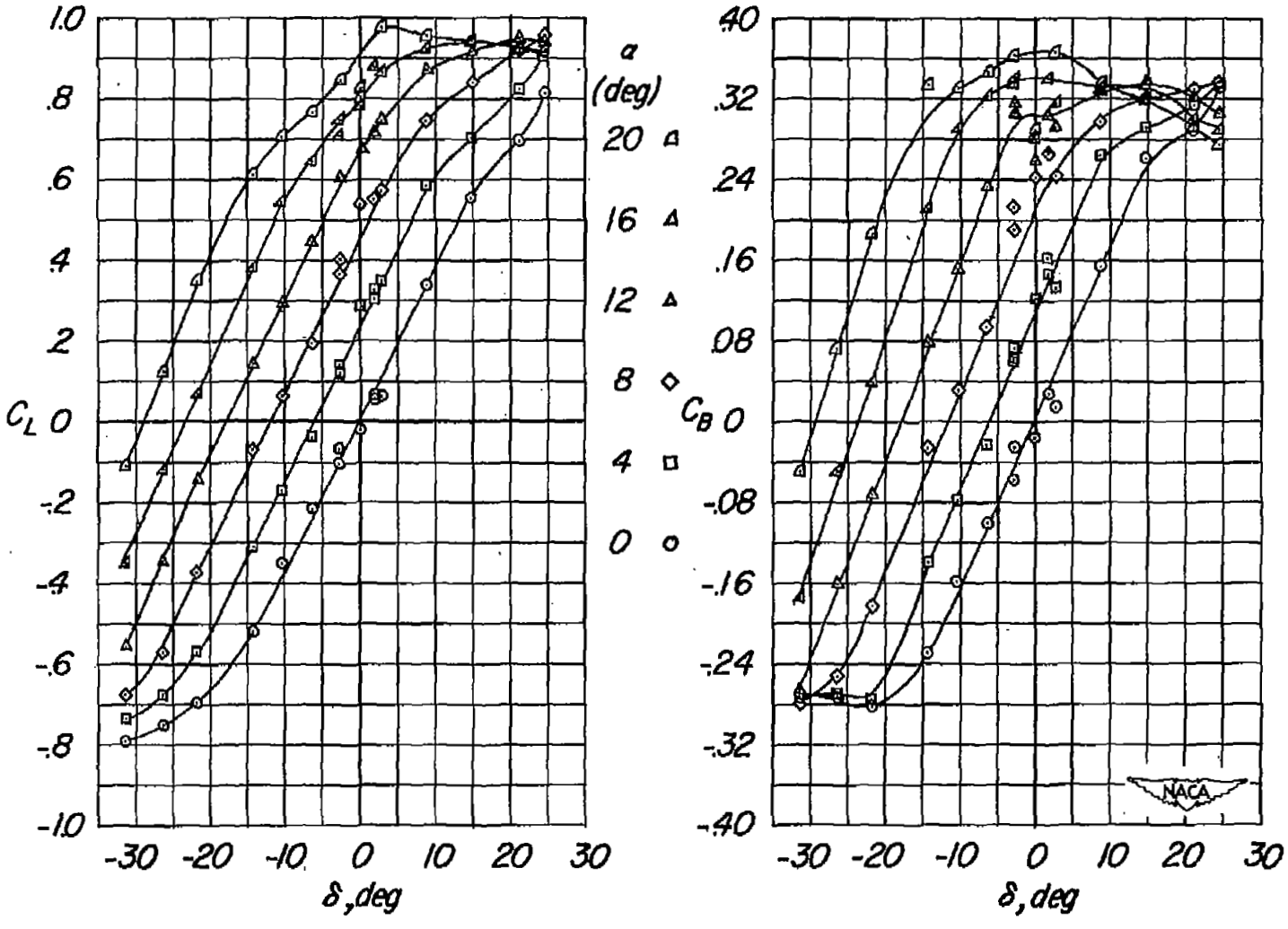

(d) Mach number, 0.975.

Figure 6.- Continued.

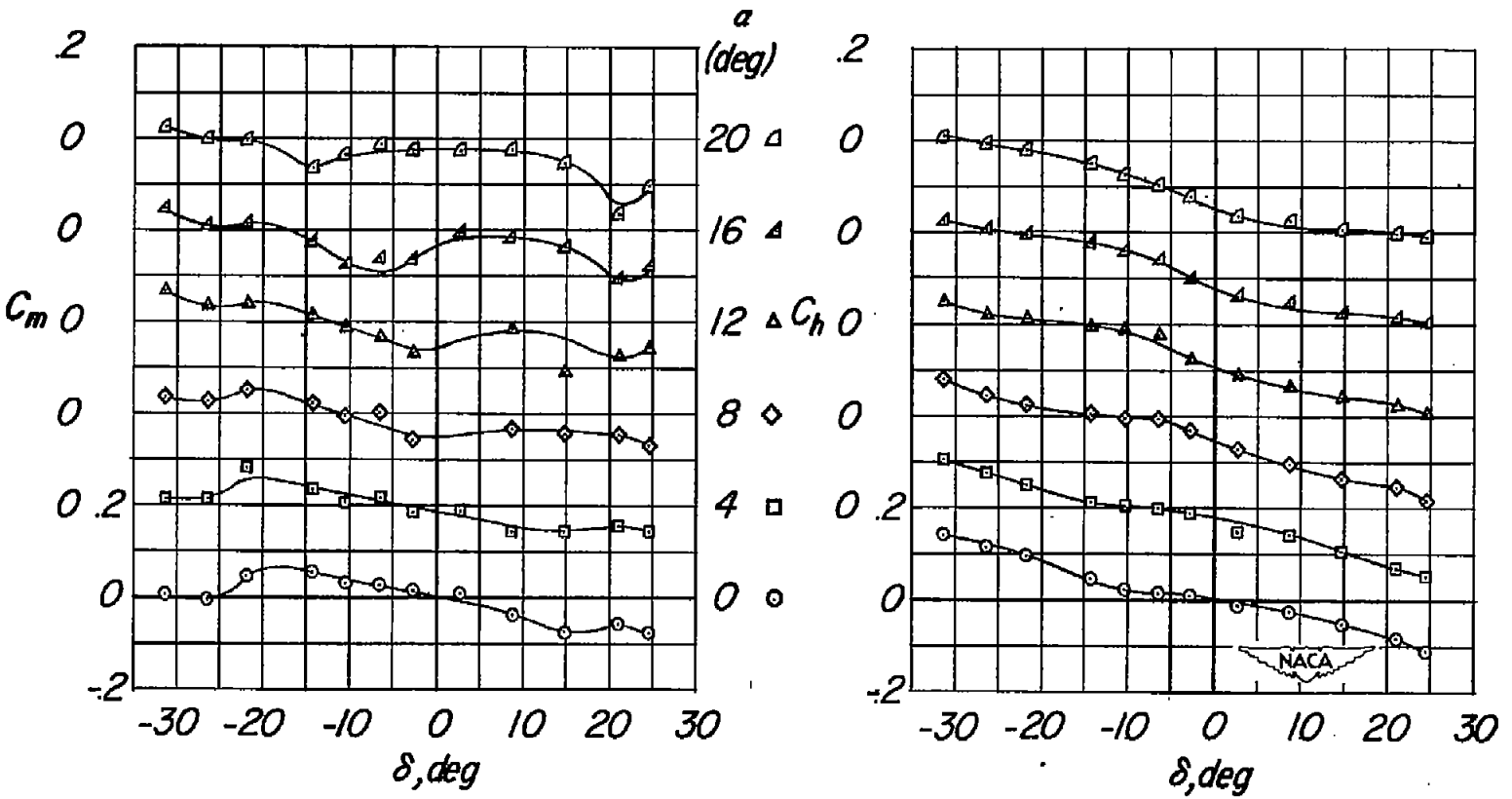

(d) Concluded.

Figure 6.- Continued.

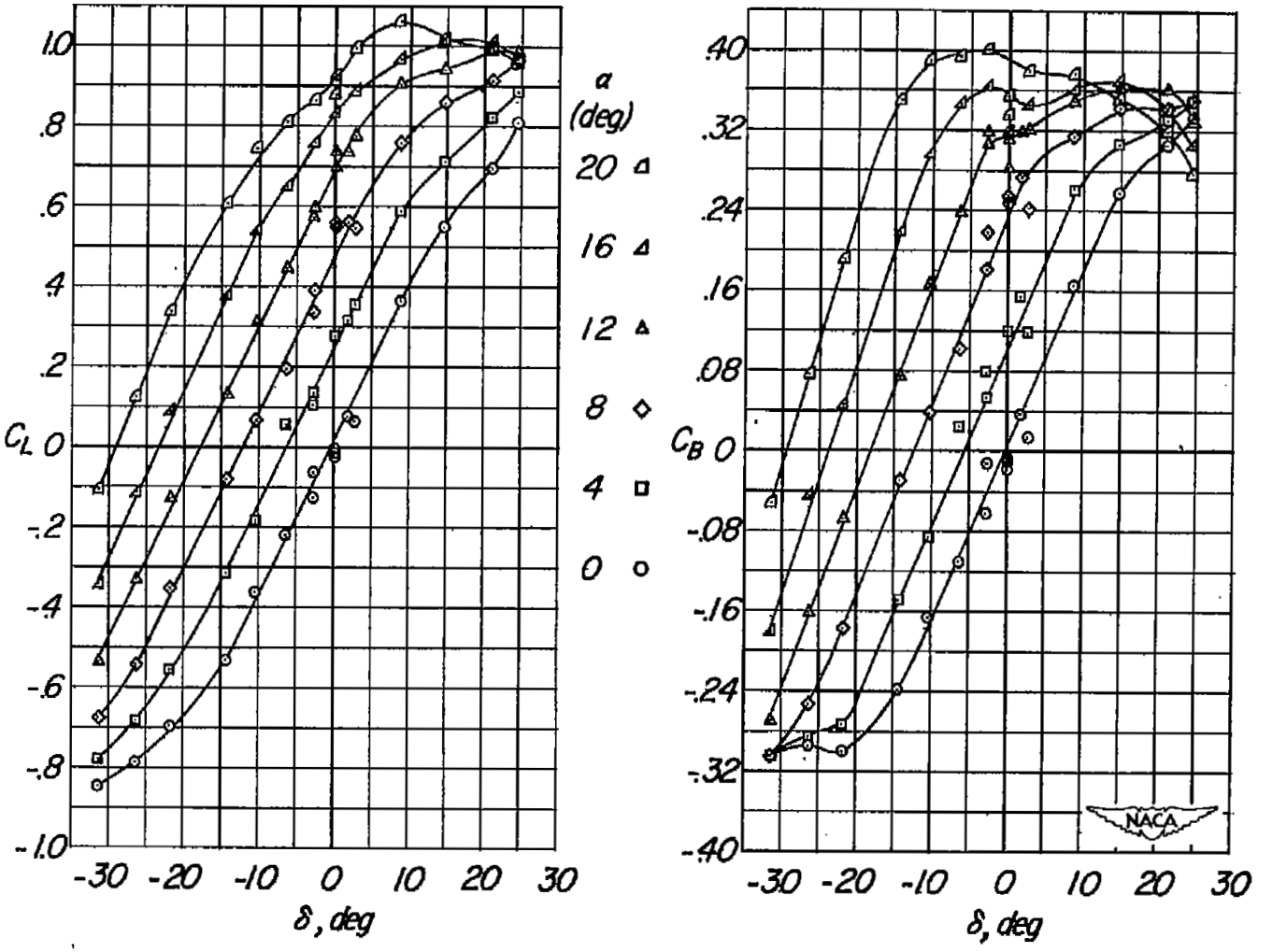

(e) Mach number, 1.027.

Figure 6.- Continued.

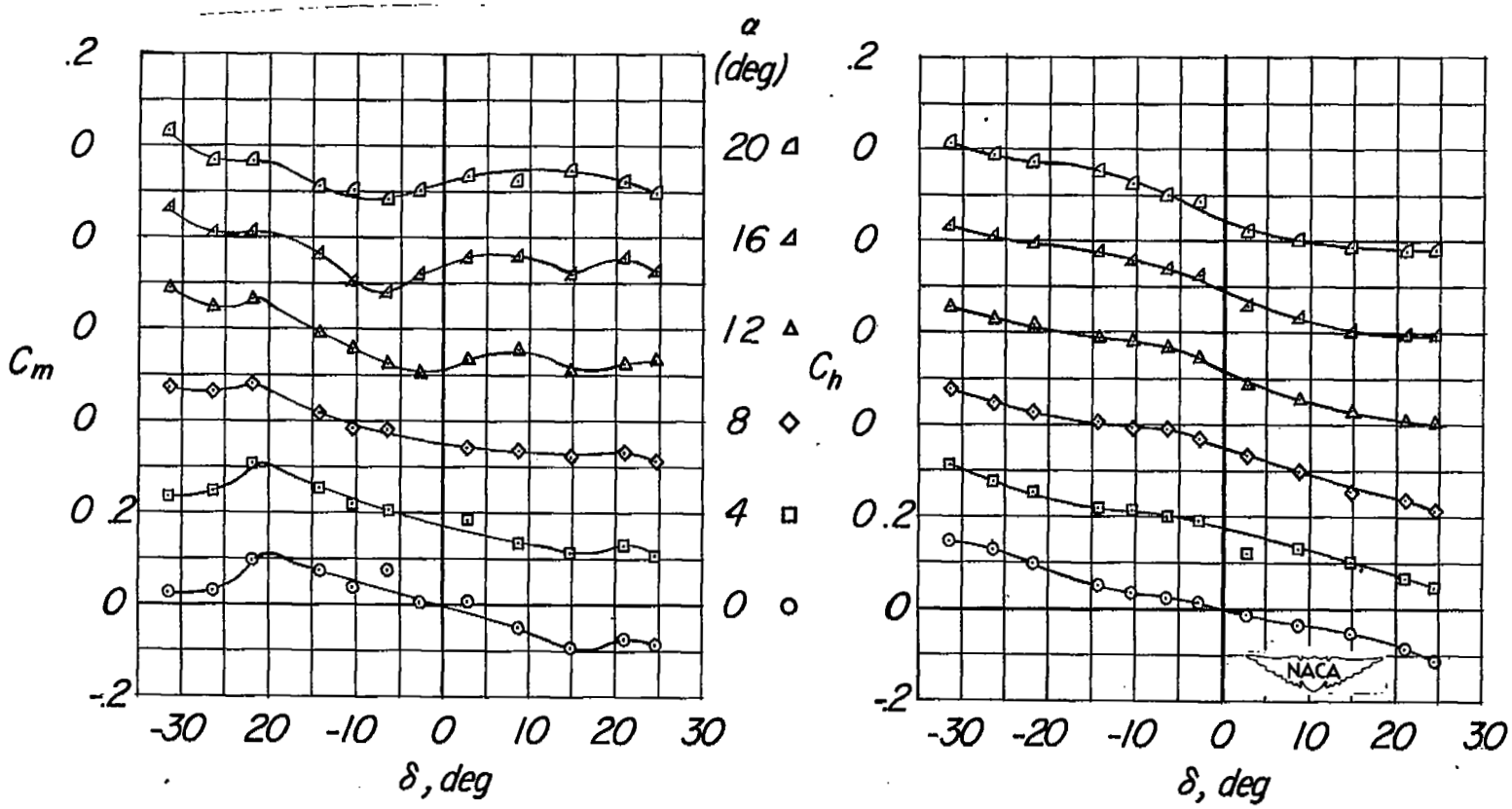

(e) Concluded.

Figure 6.- Continued.

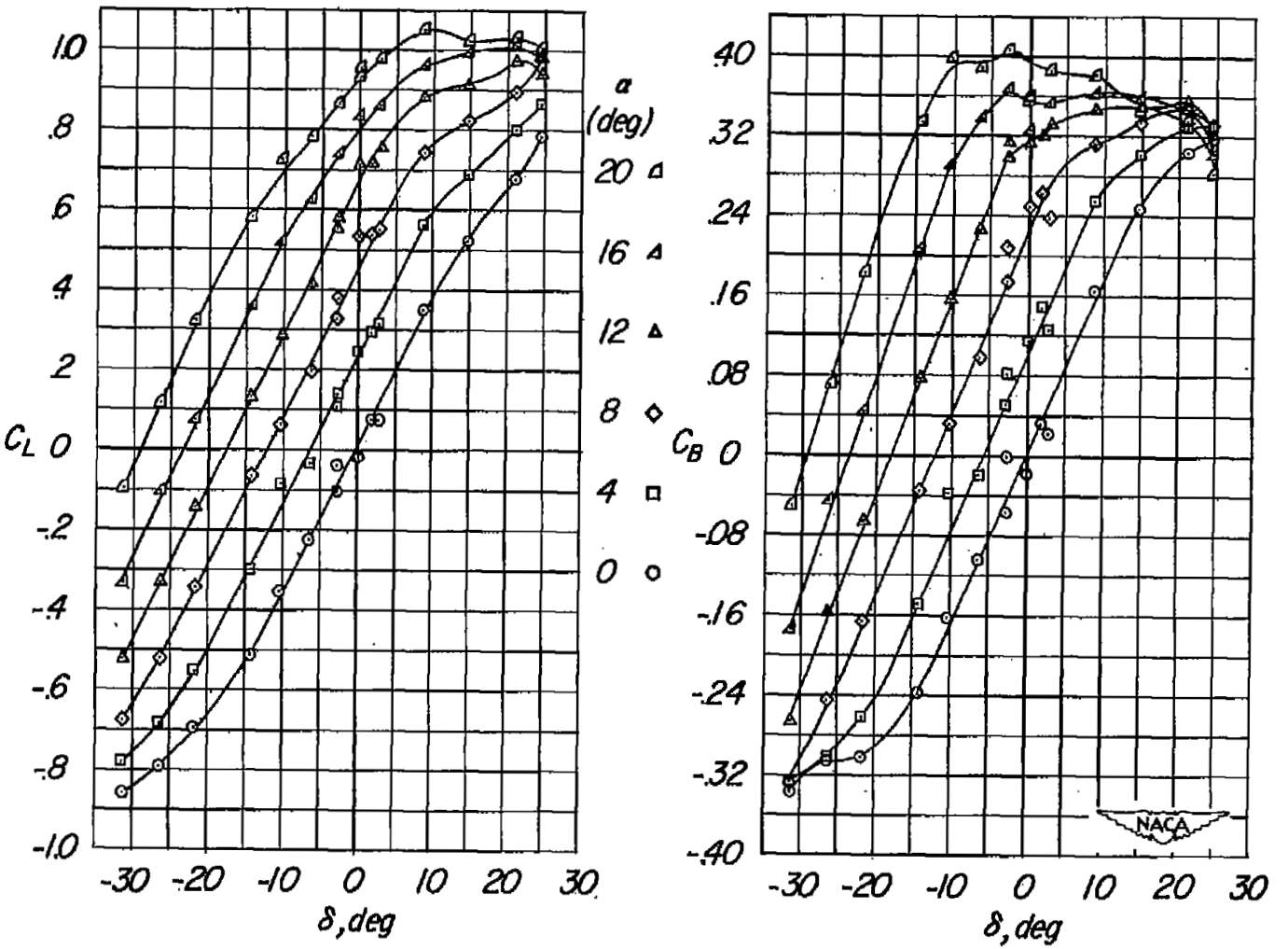

(f) Mach number, 1.058.

Figure 6.- Continued.

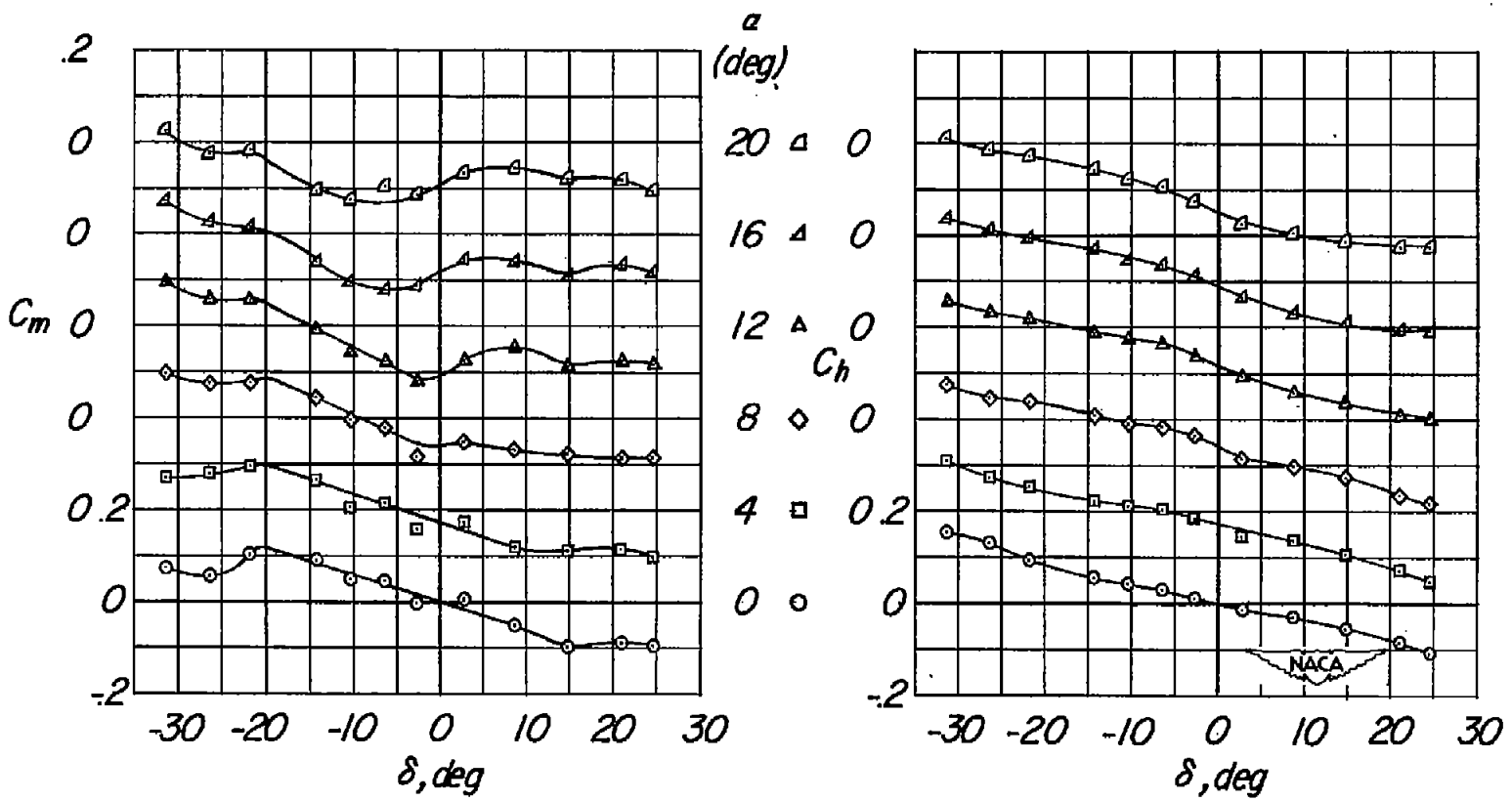

(f) Concluded.

Figure 6.- Concluded.

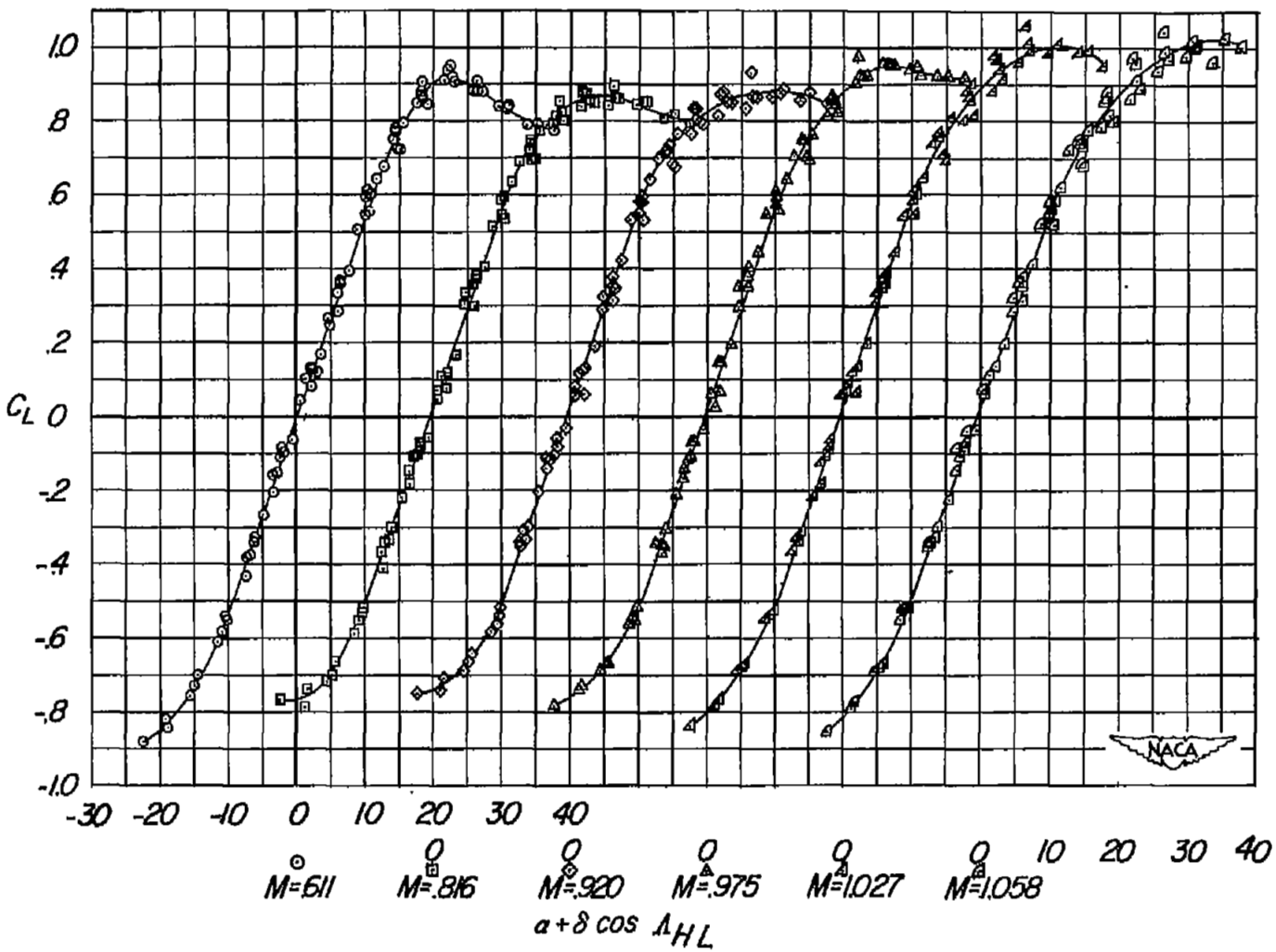

Figure 7.- The variation of lift coefficient with the parameter $\alpha + \delta \cos \Lambda_{HL}$ for the all-movable tail.

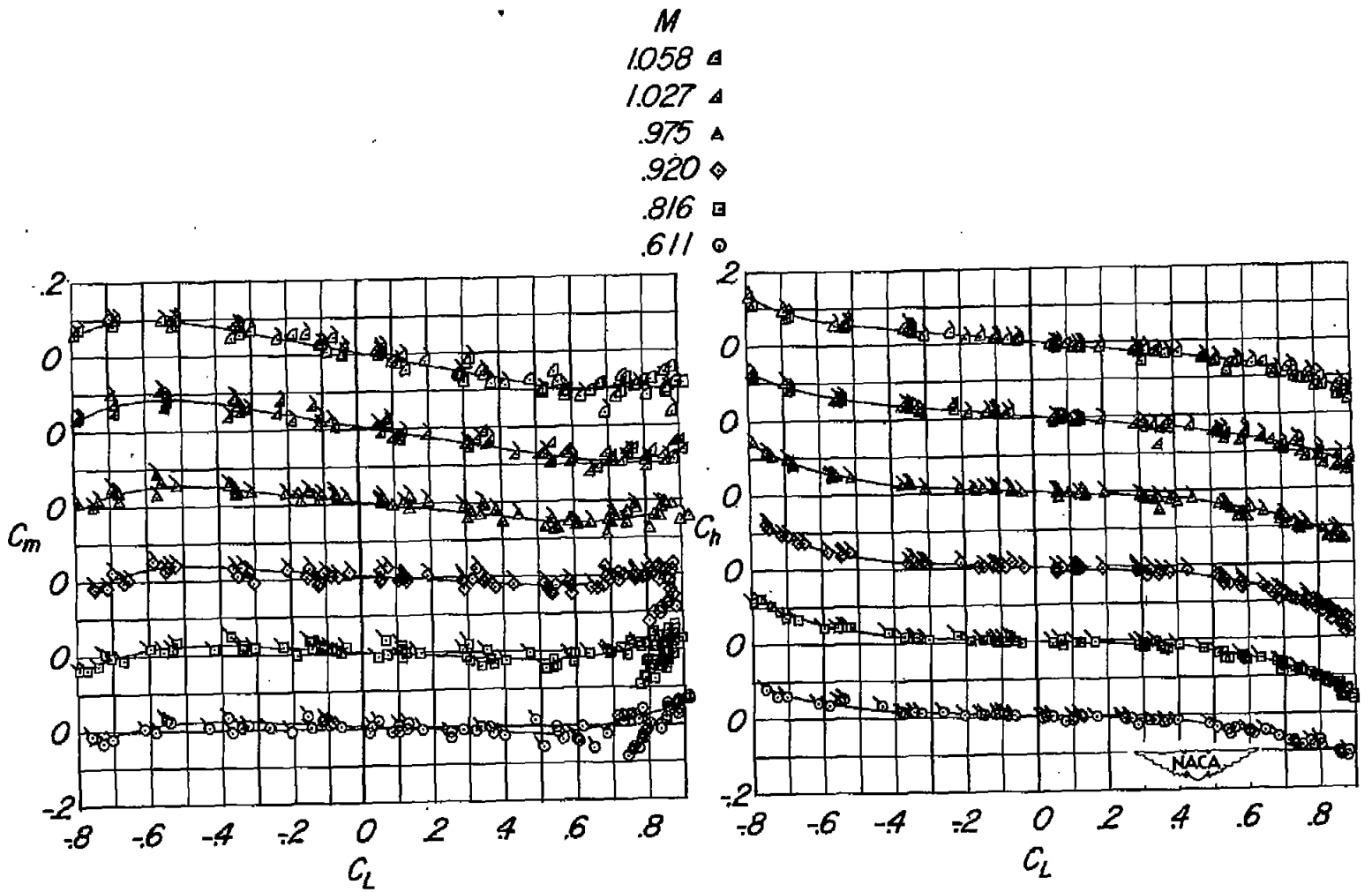

Figure 8.- The pitching-moment and hinge-moment characteristics with lift coefficient at various angles of deflection for the all-movable tail. All flagged symbols are for negative tail deflections.

$\bar{c} = 2.166$ $y_{\bar{c}} = 1.944$

Semispan = 4.242

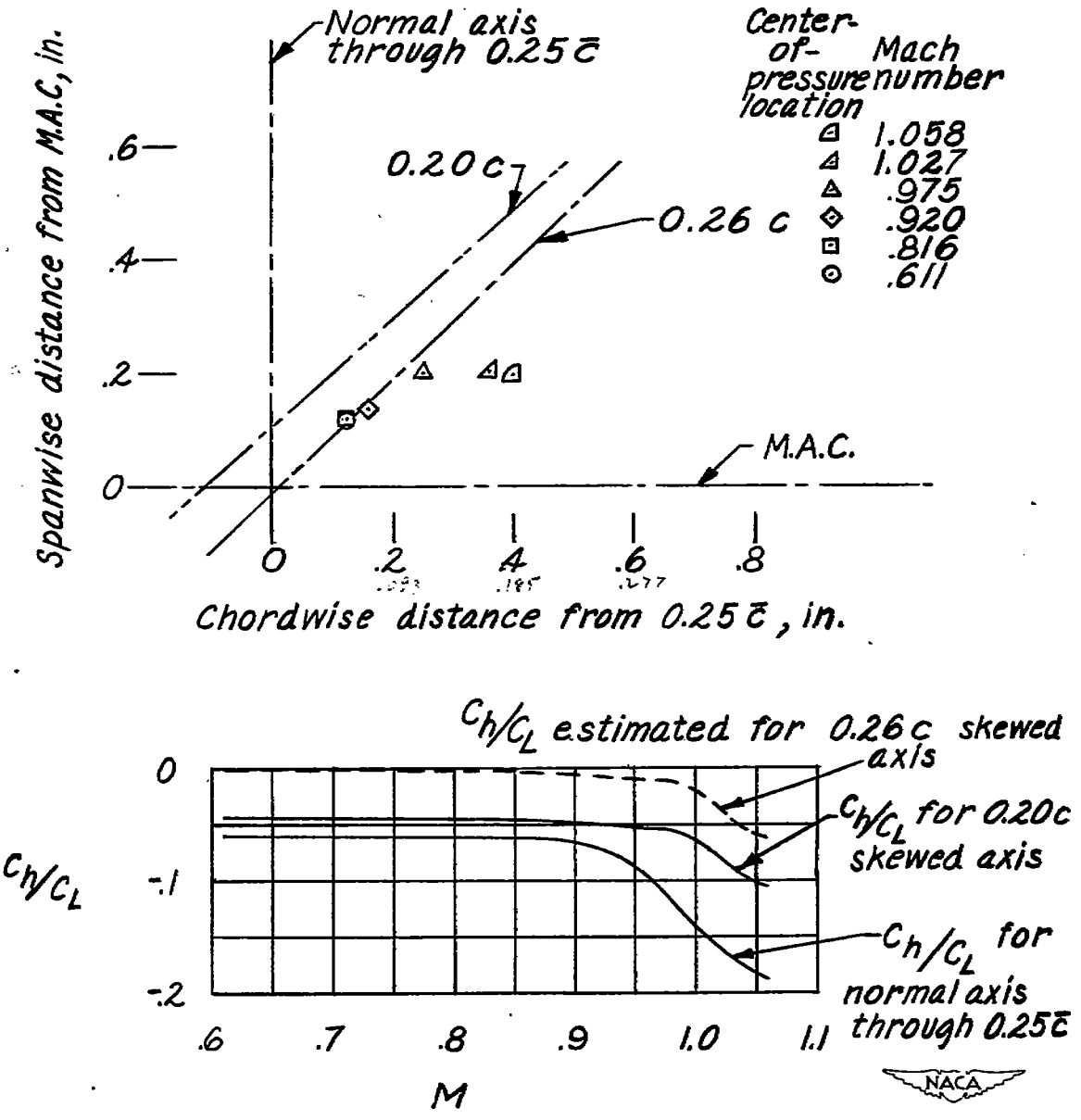

Figure 9.- The variation of the center of pressure and the parameter C_h/C_L, measured near zero lift, with Mach number for the all-movable tail.

NACA-Langley - 7-3-52 - 325